Original Paper

Developmental Neuroscience

Dev Neurosci 2003;25:403–411
DOI: 10.1159/000075666

Received: August 27, 2003
Accepted: October 3, 2003

Expression of c-*fos* in the Brain after Activation of L-Type Calcium Channels

H.A. Jinnah Kiyoshi Egami Lekha Rao MeYeon Shin Suhail Kasim
Ellen J. Hess

Department of Neurology, Johns Hopkins Hospital, Baltimore, Md., USA

Key Words
Dystonia · Self-injurious behavior · Immediate-early gene · In situ hybridization

Abstract
In rodents, administration of the L-type calcium channel activators, ±Bay K 8644 and FPL 64176, causes an unusual neurobehavioral syndrome that includes dystonia and self-injurious biting. To determine the regional influence of these drugs in the brain, the induction of c-*fos* was mapped after administration of these drugs to mice. In situ hybridization with an antisense riboprobe directed to c-*fos* mRNA revealed widespread induction, with the highest levels in the striatum, cortex, hippocampus, locus coeruleus, and cerebellum. The induction of c-*fos* mRNA was dose dependent, reached maximal expression approximately 60 min after drug treatment, and could be blocked by pretreatment with the L-type calcium channel antagonist, nifedipine. Immunohistochemical stains with an antibody directed to c-*fos* protein revealed a pattern of induction similar to that obtained with in situ hybridization in most brain regions. These results demonstrate a very heterogeneous influence of L-type calcium channel activation in different brain regions, despite the nearly universal expression of these channels implied by more classical anatomical methods.

Introduction

In rodents, blockade of L-type calcium channels with drugs such as nifedipine or nimodipine produces relatively subtle changes in behavior. These include mild reductions in locomotor activity, improved responses on learning and memory tasks, and antidepressant-like effects in forced swimming and tail suspension tests [1–3]. In comparison, activation of these channels with ±Bay K 8644 or FPL 64176 produces more obvious behavioral changes. These drugs induce a dose-dependent motor syndrome characteristic of generalized dystonia [4]. Movements become slow and stiff, and often assume a twisting quality. The L-type calcium channel activators also cause stereotypical self-biting. In weanling mice, this biting often becomes severe enough to cause tissue injury [5–7].

The biological bases for these two unusual behavioral consequences of activation of L-type calcium channels, dystonia and self-injurious biting, are not well understood. Anatomically, dystonia is most frequently associated with damage or dysfunction involving the motor pathways of the striatum. Neuropathological and neuroimaging studies of individuals with different subtypes of dystonia often reveal abnormalities in the striatum, and particularly the putamen [8]. However, dystonia can sometimes result from damage or dysfunction of other regions of the nervous system including the cortex, thalamus, midbrain, brainstem, cerebellum, spinal cord, and even peripheral nerves [8].

KARGER
Fax + 41 61 306 12 34
E-Mail karger@karger.ch
www.karger.com

0378–5866/03/0256–0403$19.50/0

Accessible online at:
www.karger.com/dne

H.A. Jinnah, MD, PhD
Department of Neurology, Meyer Room 6-181
Johns Hopkins University School of Medicine
Baltimore, MD 21287 (USA)
Tel. +1 410 614 6551, Fax +1 410 502 6737, E-Mail hjinnah@jhmi.edu

The neuroanatomical pathways responsible for self-injurious behavior are less well studied. It has been suggested that self-injurious behavior in people results from dysfunction of the non-motor pathways through the striatum since this brain region is commonly affected in clinical disorders where self-injury is observed [9]. Animal work has similarly pointed to the striatum as the source for self-injurious behavior. Intracerebral microinjections of amphetamine or the D_1-dopamine receptor agonist SKF-38393 into the ventrolateral striatum cause self-injurious biting in rats, while microinjections elsewhere do not [10, 11].

These observations on the neuroanatomical substrates for dystonia and self-injury suggest that these aspects of the neurobehavioral syndrome associated with activation of L-type calcium channels might arise from an influence of the drugs on the striatum. In the current studies, the influence of ± Bay K 8644 and FPL 64176 among different brain regions was investigated by mapping the induction of the mRNA encoding the immediate-early gene c-*fos*. Mapping the induction of c-*fos* mRNA or protein has been used extensively to examine the distribution of functionally active neurotransmitter receptors and uptake transporters, as well as the regional influence of behaviorally active drugs such as amphetamine or cocaine [12]. The results reveal that the L-type calcium channel activators induce a widespread but heterogeneous pattern of c-*fos* mRNA, with the highest levels occurring in the striatum.

Materials and Methods

Animals. C57BL/6J mice were obtained from Jackson Laboratories (www.jax.org) and maintained in the Johns Hopkins University vivarium on a 14:10 h light:dark cycle with free access to food and water. Animals were 8–10 weeks of age at the time of testing, unless otherwise noted. All animal procedures were conducted in accordance with guidelines established by the Johns Hopkins University Animal Care and Use Committee and the National Institutes of Health.

Drug Treatment. ± Bay K 8644, FPL 64176, and nifedipine were obtained from Sigma (www.sigma-aldrich.com). All drugs were dissolved in a 50:50 mixture of ethanol with Tween-80, then diluted at least 10-fold with H_2O immediately prior to injection. Injections were performed subcutaneously, in a total volume of 10 ml/kg. Each drug-treated group was evaluated in parallel with a vehicle-treated control group.

Behavior Assessment. Behaviors of drug-treated mice were assessed by direct observation for 1 min every 10 min for an hour. The severity of dystonia provoked by ± Bay K 8644 at each time point was determined using a rating scale as previously reported [4]. This severity scale is based on the level of disability and ranges from 0 to 4 (table 1). A single score for each animal was obtained by averaging all scores for the entire recording period. The number of animals with biting sufficient to cause tissue injury was also recorded [13]. If self-injury occurred, a cotton-tipped applicator was used to prevent further injury so that the experiment could proceed to the planned time point for tissue collection.

Table 1. Dystonia Rating Scale

Score	Behavior
0	Normal motor behavior
1	No impairment; slightly slowed or abnormal motor behavior
2	Mild impairment; limited ambulation unless disturbed, transient abnormal postures, infrequent falls
3	Moderate impairment; limited ambulation even when disturbed, frequent abnormal postures, frequent falls but upright for majority of time
4	Severe impairment; almost no ambulation, sustained abnormal postures, not upright for majority of time

In situ Hybridization. Brains were collected after decapitation, rapidly frozen in isopentane cooled on dry ice, and stored at –70°C until sectioning. The brains were cut with a cryostat at a thickness of 20 μm, and sections spaced at 200-μm intervals throughout each brain were thaw-mounted onto glass slides. In situ hybridization for c-*fos* mRNA was performed using a ^{35}S-labelled riboprobe as previously described, with the sense strand as a negative control [14]. Processed sections were then apposed to X-ray film to produce autoradiographic images.

Immunohistochemistry. Immunostaining for c-*fos* was performed as previously described with minor modification [15]. Mice were anesthetized with methoxyflurane and perfused transcardially with 20 ml of saline followed by 50 ml of freshly prepared 4% paraformaldehyde in 0.1 *M* phosphate buffer at pH 7.4. Brains were removed, stored in the same fixative overnight at 4°C, and then transferred to 30% sucrose in 0.1 *M* phosphate buffer for 2–4 days at 4°C. Tissue was cut on a Microm HM440E freezing microtome (www.microm.de) at a thickness of 25 μm and stored in a cryopreservative consisting of 30% ethylene glycol with 30% glycerol in 0.1 *M* phosphate butter at –20°C until staining.

Free-floating sections were rinsed free of cryopreservative and permeabilized for 30 min with 0.3% Triton X-100, 0.9% NaCl, and 50 m*M* Tris buffer at pH 7.4. Sections were then incubated for 2 days at 4°C with the PC38S polyclonal c-*fos* antiserum (www.calbiochem.com) diluted 1:20,000 in 50 m*M* Tris buffer with 1% goat serum, 0.1% Triton X-100, and 0.01% sodium azide. The secondary antibody was diluted 1:1,000 and applied for 2 h at 24°C. The stain was developed using the avidin-biotin complex method with alkaline phosphatase and Vector Red as the chromogen (www.vectorlabs.com). In some cases, a cresyl violet counterstain was applied.

Data Analysis. Two levels of analysis were applied to the in situ hybridization results to compare the relative optical density of images of drug-treated animals to that of the simultaneously processed tissue from control animals treated with vehicle only. The first level consisted of a single rater scoring multiple regions throughout the entire brain with a semiquantitative scale to rate the density of labeling: 0 = none, + = minor, ++ = moderate, +++ = heavy. These data served as a screening tool; they were not quantitatively analyzed.

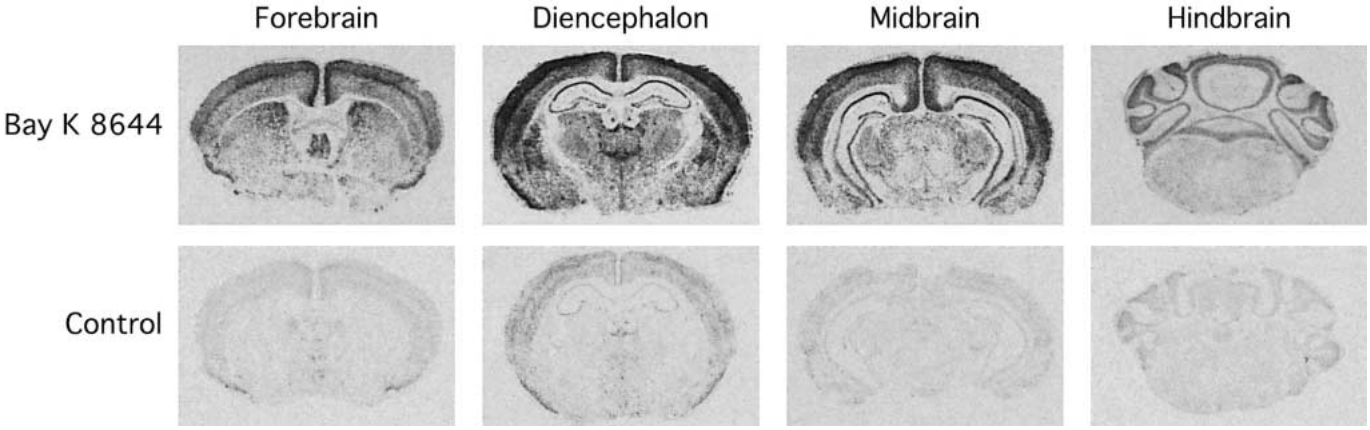

Fig. 1. Distribution of c-*fos* mRNA after ± Bay K 8644. The top row shows representative autoradiograms from four brain regions 30 min after 4 mg/kg ± Bay K 8644. The bottom row shows autoradiograms from animals treated with vehicle only (n = 4 animals for each group).

The second level consisted of quantitative densitometry applied to several representative regions that displayed relatively high levels of label. The MCID Elite imaging analysis system (www.imaging research.com) was used to capture a digital image of the counterstained slide, superimpose the corresponding autoradiographic images, and determine the optical density of autoradiographic grains for each region of interest. Experimental variability in this technique comes from a variety of sources including the specific activity of the radiolabeled probe, the efficiency of the hybridization reaction, tissue treatments to reduce non-specific background, inherent differences in background among brain regions, and film exposure and development conditions. Results were therefore expressed as a percentage of the corresponding region from a simultaneously processed control group to limit many of these sources of variability to produce an intra-assay variability of $<10\%$. For statistical comparisons, ANOVA was applied to the raw optical density measures, with post-hoc Tukey t-tests where appropriate.

Results

Regional Distribution

The regional induction of c-*fos* mRNA was first examined 30 min after 4 mg/kg ± Bay K 8644 (fig. 1, table 2). In the hindbrain, the most prominent expression was observed in the locus coeruleus and cerebellum. Only minor expression was observed in most of the midbrain; the substantia nigra was notably devoid of label. Many areas were labeled in the forebrain including cortex, hippocampus, striatum, and certain thalamic and hypothalamic nuclei. A laminar distribution was observed in the cortex, with the heaviest labeling in layer 5 and little or no labeling in layer 1. Expression in the striatum was similarly heterogeneous, with more in the dorsomedial in comparison to the ventrolateral portion.

Dose Response

The induction of c-*fos* mRNA was next examined 30 min after 0, 2, 4, or 8 mg/kg ± Bay K 8644. A dose-dependent influence on the intensity of expression was evident within most regions examined (fig. 2). Maximum induction was observed in the dorsomedial striatum, where expression reached 554% of vehicle-treated controls. In contrast, maximal induction in most other areas fell in the 200–300% range.

Time Course

To determine the temporal profile for induction of c-*fos* mRNA, mice were treated with vehicle or 4 mg/kg ± Bay K 8644 and tissue was collected at 0, 30, 60, 90, 120 and 240 min. The c-*fos* induction reached a maximum in 1–2 h and returned to baseline by 4 h in most brain regions (fig. 3). The one exception was the locus coeruleus, where expression remained high for at least 4 h.

Pharmacologic Specificity

Because the time course experiment suggested that a higher signal was achieved at 60 min rather than at 30 min, subsequent experiments employed the longer time point. To investigate the pharmacological specificity of c-*fos* mRNA induction, the effects of an alternative L-type calcium channel activator (FPL 64176) and pretreatment with an L-type calcium channel antagonist (nifedipine) were examined. Pretreatment with 10 mg/kg nifedi-

Table 2. Regional c-*fos* mRNA expression

Brain region		Relative signal
Telencephalon	Cortex	
	Neocortex	++
	Cingulate cortex	+++
	Entorhinal cortex	++
	Corpus callosum	0
	Medial preoptic area	0
	Bed nuclei stria terminalis	+
	Amygdala	+
	Hippocampus	
	Corpus Amonus	+++
	Dentate gyrus	++
	Molecular layer	0
	Striatum	
	Dorsomedial	+++
	Ventrolateral	++
	Globus pallidus	+
	Accumbens	+
Diencephalon	Thalamus	
	Ventromedial	++
	Dorsomedial	+
	Medial habenula	0
	Ventral posterior	+
	Paraventricular	++
	Medial geniculate	++
	Lateral geniculate	+
	Hypothalamus	
	Supraoptic nuclei	+
	Anterior hypothalamus	++
	Ventromedial hypothalamus	+
Mesencephalon	Substantia nigra	0
	Ventral tegmentum	0
	Superior colliculus	+
	Inferior colliculus	+
	Periaqueductal gray	+
	Oculomotor nucleus	+
Rhombencephalon	Locus coeruleus	+++
	Pons	++
	Dorsal raphe	0
	Trigeminal nucleii	0
	Nucleus ambiguous	0
	Cerebellum	
	Granule cell layer	+++
	Purkinje cell layer	+
	Molecular layer	0

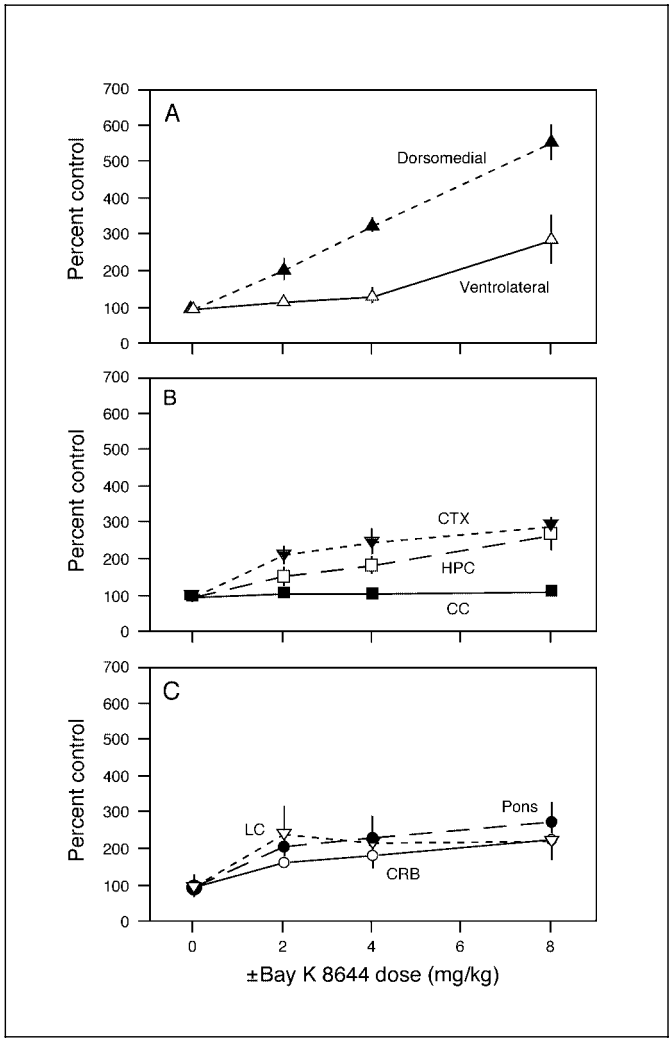

Fig. 2. Dose response for c-*fos* mRNA induction. For each dose, brains were collected from 4 mice treated with ±Bay K 8644 and 4 mice treated with vehicle only. Results represent average optical density ± SEM expressed as a percentage of the vehicle-treated control group. In some cases, the error bars appear missing because they were smaller than the symbol used for the data point. The raw optical density measures were analyzed by two-way ANOVA, with drug dose and brain region as the main variables. This analysis revealed significant effects for both drug dose ($F_{3,95}$ = 46.6, $p < 0.001$) and brain region ($F_{7,95}$ = 13.0, $p < 0.001$). Regions shown include (**A**) dorsomedial striatum (▲), ventrolateral striatum (△); (**B**) hippocampus (□), cortex (▼), corpus callosum (■); and (**C**) locus coeruleus (▽), cerebellum (○), and pons (●).

pine 10 min before 4 mg/kg ±Bay K 8644 produced patterns and intensity of induction indistinguishable from vehicle-treated controls in all areas (fig. 4). Treatment with 4 mg/kg FPL 64176 produced a pattern of labeling similar to that of 4 mg/kg ±Bay K 8644. With the exception of the locus coeruleus, the intensity of label with FPL 64176 was lower than that of ±Bay K 8644 in all regions (fig. 4). The lower levels of expression with FPL 64176 are in keeping with the lower potency of this drug in behavioral studies [4, 5].

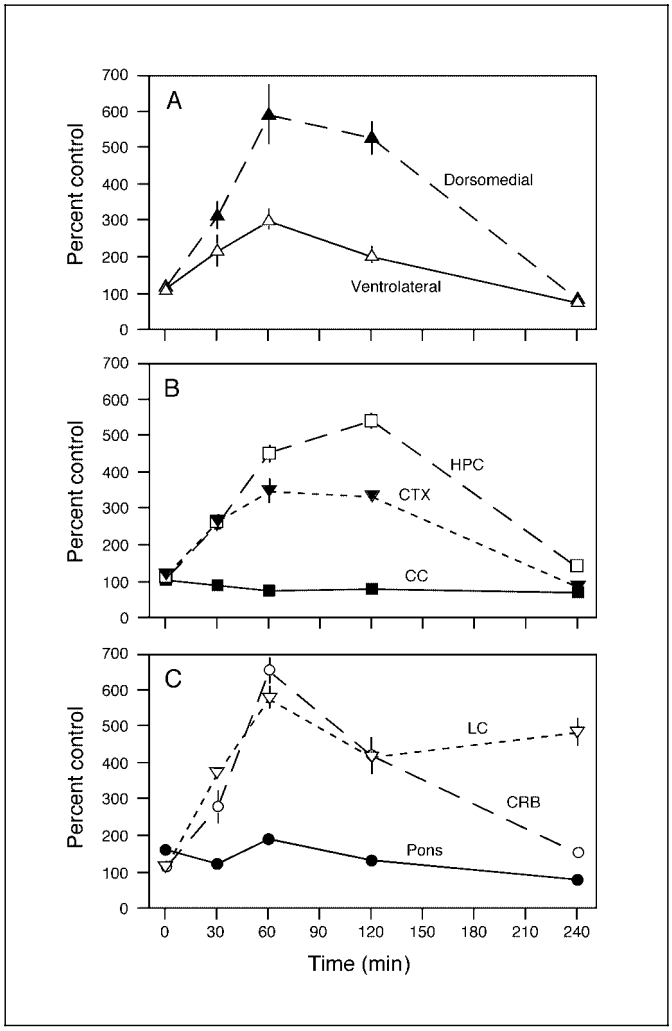

Fig. 3. Time course for c-*fos* mRNA induction. For each time point, brains were collected from 3 mice treated with 4 mg/kg ± Bay K 8644 and 3 mice treated with vehicle only. Results represent average optical density ± SEM expressed as a percentage of the vehicle-treated control group. In some cases, the error bars appear missing because they were smaller than the symbol used for the data point. The raw optical density measures were analyzed by ANOVA, with drug treatment, time, and brain region as main variables. This analysis revealed significant effects for drug treatment ($F_{1,160}$ = 943.2, $p < 0.001$), time ($F_{4,160}$ = 147.5, $p < 0.001$), and brain region ($F_{7,160}$ = 66.0, $p < 0.001$). Regions shown include (**A**) dorsomedial striatum (▲), ventrolateral striatum (△); (**B**) hippocampus (□), cortex (▼), corpus callosum (■); and (**C**) locus coeruleus (▽), cerebellum (○), and pons (●).

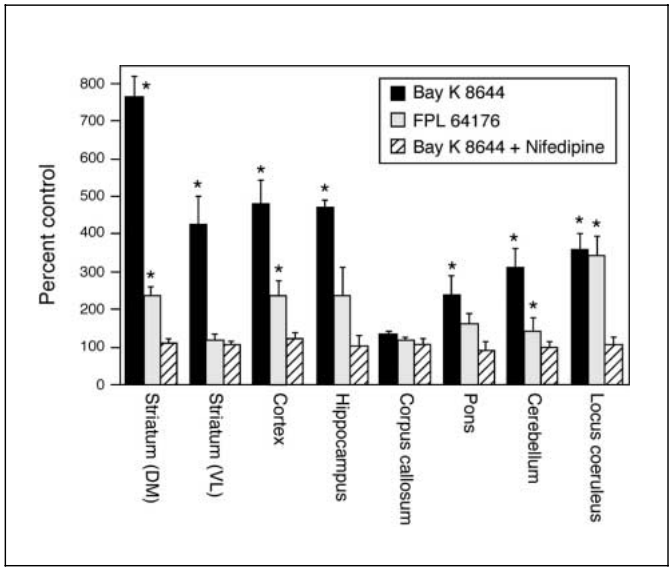

Fig. 4. Pharmacologic specificity of c-*fos* mRNA induction. Brains were collected from 4 mice for each treatment condition: 4 mg/kg ± Bay K 8644 (black bars), 4 mg/kg FPL 64176 (open bars), 10 mg/kg nifedipine 10 min prior to 4 mg/kg ± Bay K 8644 (hatched bars), and vehicle only. Results represent average optical density ± SEM expressed as a percentage of the vehicle-treated control group. The raw optical density measures were analyzed by two-way ANOVA, with treatment group and brain region as the main variables. This analysis revealed significant effects for both treatment group ($F_{3,80}$ = 140.1, $p < 0.001$) and brain region ($F_{7,80}$ = 13.9, $p < 0.001$). The asterisks depict significant differences from the vehicle-treated control group as determined by post-hoc Tukey tests ($p < 0.05$).

Influence of Animal Age

Previous studies have documented considerable changes in the density of calcium channels and the behavioral consequences of ± Bay K 8644 in weanling versus adult mice [4, 5, 16]. The induction of c-*fos* mRNA was therefore compared in weanling (4–5 weeks of age) and adult mice (8–10 weeks of age) to look for regional differences in the pattern or intensity of labeling 60 min after drug delivery. The overall patterns of label were similar, but the intensity of the label was higher in weanling in comparison to adult mice in most brain regions (fig. 5). The differences between the age groups were more pronounced in particular regions. The ventrolateral striatum demonstrated the most prominent differences between weanling and adult mice. In this region, weanling mice displayed a 389% increase in labeling relative to vehicle-treated weanling controls, while adult mice displayed a 59% increase that was not statistically different from the vehicle-treated controls. In contrast, the induction of c-*fos* mRNA was similar in weanling and adult mice in other regions such as the hippocampus (fig. 5).

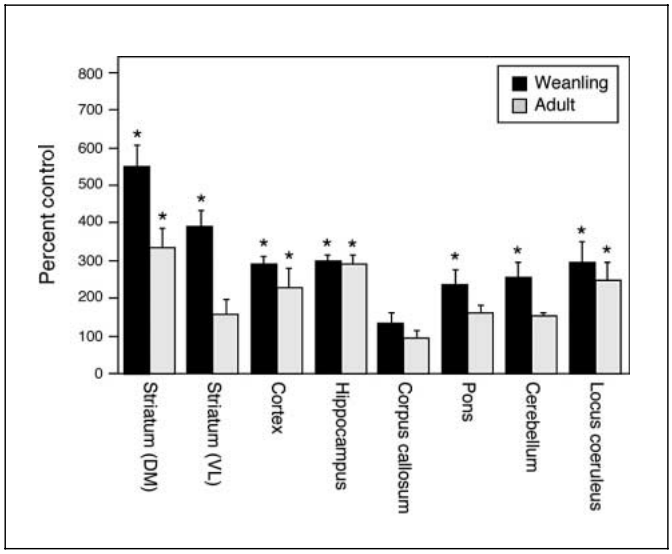

Fig. 5. Influence of age on c-*fos* mRNA induction. Brains were collected from 4 weanling and 4 adult mice treated with 4 mg/kg ± Bay K 8644. Separate groups of 4 weanling and adult mice were treated with vehicle only. Results represent average optical density ± SEM expressed as a percentage of the vehicle-treated control group. The raw optical density measures were analyzed by ANOVA, with drug treatment, age, and brain region as the main variables. This analysis revealed significant effects for drug treatment ($F_{1,96}$ = 279.8, $p < 0.001$), age ($F_{1,96}$ = 42.1, $p < 0.001$) and brain region ($F_{7,96}$ = 12.9, $p < 0.001$). The asterisks depict significant differences from the associated vehicle-treated control group as determined by post-hoc Tukey tests ($p < 0.05$).

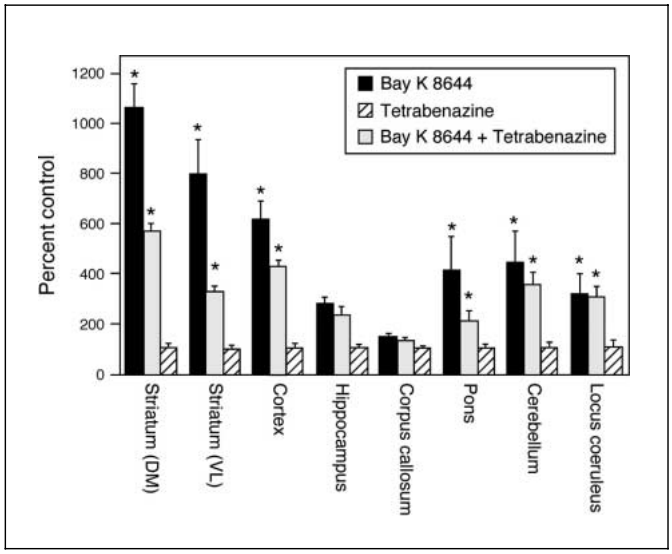

Fig. 6. Pharmacologic modifiers of c-*fos* mRNA induction. Brains were collected from 3 mice for each treatment condition: 6 mg/kg ± Bay K 8644 (black bars), 5 mg/kg tetrabenazine (open bars), 5 mg/kg tetrabenazine 10 min prior to 6 mg/kg ± Bay K 8644 (hatched bars), and vehicle only. Results represent average optical density ± SEM expressed as a percentage of the vehicle-treated control group. The raw optical density measures were analyzed by two-way ANOVA, with treatment group and brain region as the main variables. This analysis revealed significant effects for both treatment group ($F_{3,64}$ = 86.6, $p < 0.001$) and brain region ($F_{7,64}$ = 14.3, $p < 0.001$). The asterisks depict significant differences from the vehicle-treated control group as determined by post-hoc Tukey tests ($p < 0.05$).

Table 3. Behavioral effects of tetrabenazine

Treatment condition	Self-injury % mice	Dystonia average score
Vehicle only (n = 5)	0	0.5 ± 0.2
5 mg/kg tetrabenazine only (n = 5)	0	0.6 ± 0.1
6 mg/kg ± Bay K 8644 only (n = 5)	100	2.9 ± 0.1*
Tetrabenazine plus ± Bay K 8644 (n = 4)	0	3.5 ± 0.1*,†

The percentages of mice with self-injury were not compared statistically, but the dystonia scores were subjected to ANOVA with post-hoc Tukey t-tests. * Significant difference ($p < 0.05$) from the control (vehicle) group; † Significant difference between the groups given ± Bay K 8644 alone versus ± Bay K 8644 with tetrabenazine.

Pharmacological Modifiers

A previous study showed that pretreatment of mice with the dopamine-depleting agent tetrabenazine 10 min before ± Bay K 8644 eliminates self-injurious biting [13]. Pretreatment with 5 mg/kg tetrabenazine was confirmed to reduce self-injurious biting in response to 6 mg/kg ± Bay K 8644 while simultaneously exaggerating the dystonia (table 3). Because of the opposing effects of tetrabenazine on self-injury and dystonia, its influence on the regional induction of c-*fos* mRNA was examined. Tetrabenazine alone caused no detectable changes in c-*fos* mRNA levels in any brain region. However, it significantly reduced the ability of ± Bay K 8644 to induce c-*fos* mRNA in most brain regions examined (fig. 6).

Immunohistochemistry

Several controls were used to verify the specificity of labeling observed with the in situ hybridization method, including the use of the opposing sense strand mRNA and

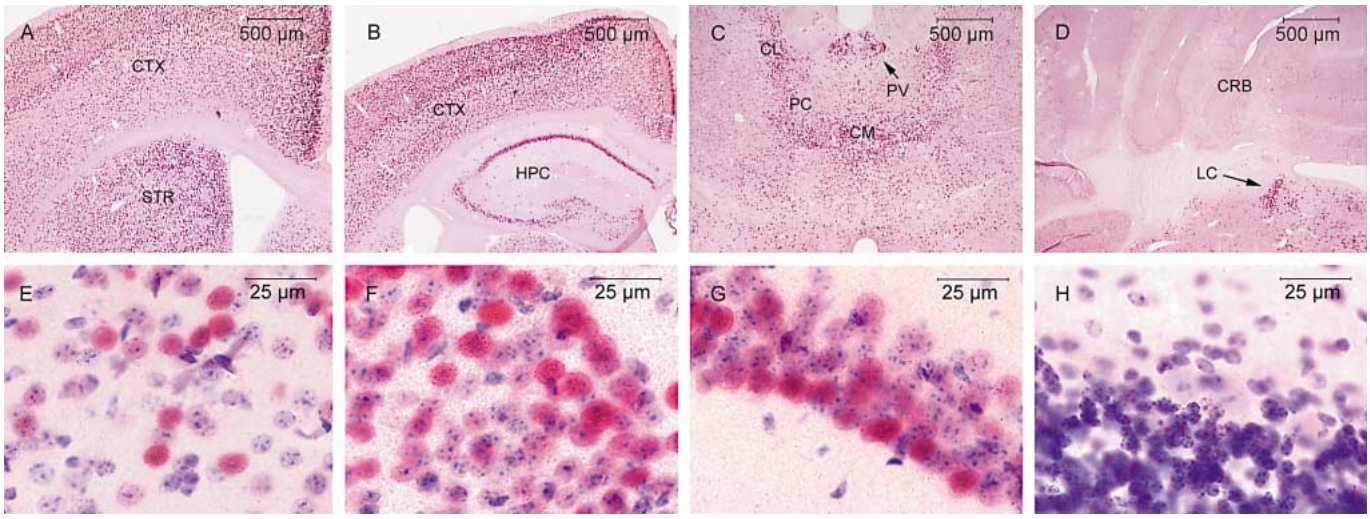

Fig. 7. Localization of c-*fos* immunoreactivity. Immunohistochemistry was conducted on brain tissue collected from 4 mice 60 min after 4 mg/kg ± Bay K 8644 or vehicle. Low power magnifications demonstrate the regional distribution of c-*fos* immunostaining for dorsomedial striatum and overlying cerebral cortex (**A**); hippocampus and overlying cerebral cortex (**B**); thalamus at the level of the third ventricle (**C**), and cerebellum with locus coeruleus (**D**). Higher power magnifications demonstrate the nuclear distribution of the Vector Red chromogen labeling the c-*fos* antigen against a light purple background of a cresyl violet counterstain for the dorsomedial striatum (**E**); cerebral cortex (**F**); CA1 of the hippocampus (**G**), and interface between the molecular and granule cell layers of the cerebellum (**H**). CL = Centrolateral nucleus of the thalamus; CM = centromedian nucleus of the thalamus; CRB = cerebellum; CTX = cortex; HPC = hippocampus; LC = locus coeruleus; PC = paracentral nucleus of the thalamus; PV = paraventricular nucleus of the thalamus; STR = striatum.

pretreatment of sections with RNase, as previously described [14]. As an independent method, immunohistochemical stains for c-*fos* antigen were also examined at 200-µ*M* intervals throughout the brain.

As previously described, the immunostains for c-*fos* resulted in intense labeling of specific nuclei [15]. The pink c-*fos* immunolabel resulting from the Vector Red stain could be easily discriminated from the darker blue-purple cresyl violet counterstain that labeled all nuclei (fig. 7). The pink-stained nuclei observed 60 min after 4 mg/kg ± Bay K 8644 were qualitatively observed to occur in a distribution similar to that observed with the in situ hybridization method, but the percentage of immunolabeled nuclei was not quantitatively further evaluated. There was one notable discrepancy between the immunohistochemical and in situ hybridization findings. Cerebellar granule cells were devoid of any detectable immunolabeling (fig. 7), but were clearly labeled with the antisense mRNA probe (fig. 1).

Discussion

The current results revealed that induction of c-*fos* mRNA after pharmacological activation of the L-type calcium channels occurred with a broad distribution in the mouse brain. The highest levels of induction were observed in the striatum, cortex, hippocampus, specific thalamic and hypothalamic nuclei, the locus coeruleus, and the cerebellum. There was a heterogeneous induction of c-*fos* within some regions. For example, the cerebral cortex displayed a laminar distribution, while the striatum demonstrated significant variation among dorsomedial and ventrolateral regions.

*Correlation between c-*fos *Induction and Neurobehavioral Syndrome*

The widespread induction of c-*fos* after administration of ± Bay K 8644 makes it difficult to make any correlations among the brain regions affected and the associated neurobehavioral syndrome. However, it is interesting to note that the most intense c-*fos* induction was consistently observed in the dorsomedial striatum. As previously noted, dystonia is a prominent motor consequence of

administering the L-type calcium activators to mice, and the striatum has most often been implicated as the source of dystonia in other studies [8]. It is impossible to say with confidence that ± Bay K 8644 causes dystonia by an influence on this region, however, because multiple other brain regions involved in motor control were also influenced by ± Bay K 8644.

Significant c-*fos* mRNA was also induced by ± Bay K 8644 in the ventrolateral striatum, the region implicated in the expression of self-injurious behavior [9]. In fact, the induction of c-*fos* in this region was observed predominantly under conditions known to be associated with this specific behavior. The c-*fos* induction in this region occurred only with relatively high doses of ± Bay K 8644, in keeping with observations that self-biting occurs only with relatively high doses [5]. In addition, the induction of c-*fos* in this region was much more robust in weanling than adult mice, an observation consistent with prior observations that self-biting is much more frequent and severe in younger animals [5]. Finally, the L-type calcium channel activators differ in their ability to provoke stereotypical self-biting. The behavior is prominent with ± Bay K 8644 but uncommon with FPL 64176 [5]. While ± Bay K 8644 induced c-*fos* in both the dorsomedial and ventrolateral striatum, FPL 64176 induced c-*fos* only in the dorsomedial striatum. These observations confirm the original hypothesis that ± Bay K 8644 may cause dystonia and self-biting by an influence on the striatum.

Anatomical Maps of L-Type Calcium Channels

The distribution of c-*fos* mRNA observed after the administration of ± Bay K 8644 is largely consistent with the distribution of L-type calcium channels identified with other anatomical methods. In situ hybridization studies of the mRNAs encoding the α_{1c} and α_{1d} subunits have revealed high levels of expression in the olfactory bulbs, hippocampus, superior colliculus, and cerebellum. Lower levels of the mRNA were found in the cortex, thalamus, and hypothalamus [17, 18]. Immunohistochemical studies with antibodies directed to L-type channels have revealed high levels of antigen in the cortex, hippocampus, striatum, and cerebellum [19, 20]. The dihydropyridine-binding site of the L-type channel has been labeled with a number of different ligands, with most studies showing high levels in the cortex, hippocampus, striatum, and cerebellum [21–23]. Lower concentrations of the binding site were also detected in other regions, including the thalamus, midbrain, and brainstem.

The different methods used to map L-type calcium channels in the brain have provided similar, though not identical results. The lack of complete concordance among the methods is likely to reflect differences in the sensitivity and specificity of the methods, as well as differences inherent in the endpoint studied. For example, the results from in situ hybridization and immunohistochemical studies may differ because of transportation of the protein product to sites distant from the location of mRNA transcript. Differences between immunohistochemical and radioligand binding may reflect variable accessibility of the antigenic or dihydropyridine-binding sites among channels located at different subcellular sites.

Functional Maps of L-Type Calcium Channels

There are several reasons to believe that induction of c-*fos* mRNA after the administration of ± Bay K 8644 provides an indirect estimate of the distribution and density of functionally active L-type channels. These channels are known to be tightly coupled to induction of c-*fos* and other immediate-early genes [24], so activation of these channels is likely to provoke a rapid induction of c-*fos*. The induction of c-*fos* after ± Bay K 8644 was blocked by pretreating animals with the L-type calcium channel antagonist nifedipine, confirming that activation of the channels was responsible for inducing the mRNA. In addition, the pattern of induction observed with ± Bay K 8644 was similar to that of FPL 64176, another L-type calcium channel agonist. The reproduction of similar patterns of c-*fos* induction by two structurally dissimilar L-type calcium channel activators increases the likelihood that the results observed are due to activation of these channels and not some nonspecific side effect of either drug. Significant c-*fos* induction was not observed in tissue examined with the mRNA sense strand as a probe, in tissue pretreated with RNase, or in simultaneously processed tissue from vehicle-treated control animals. Taken together, these results suggest that the expression of c-*fos* mRNA is specific to the effects of ± Bay K 8644.

While the maps for L-type calcium channels derived from classical methods are largely consistent with the current results that rely on functional activation of the channels, some differences are apparent. There are two main reasons why these maps may differ. First, the classical anatomical methods that identify the channel mRNA and protein do not reveal the distribution of functionally active channels. The immunohistochemical and ligand-binding methods both label membrane-bound and intracellular channels. Intracellular channels are probably not functionally active, but may represent pools of reserve channels or channels internalized as part of the normal turnover of membrane proteins [20, 25, 26]. Mapping the

induction of c-*fos* mRNA after the administration of ±Bay K 8644 reveals only functionally active calcium channels in the brain.

The second reason the anatomical and functional maps may differ is that c-*fos* may be induced by a wide variety of stimuli that influence neural activity [12], making it difficult to discriminate regions activated directly by stimulating L-type calcium channels from those secondarily activated via downstream connections. This limitation can be addressed by examining the time course of c-*fos* mRNA induction [14]. Since signals from in situ hybridization are not readily detectable until 10–15 min after a stimulus, the temporal profile of induction provides a way to separate regions activated early versus late. In the current studies, c-*fos* mRNA induction was observed at the earliest time point examined and peaked by 60 min in most brain regions. This time course is consistent with the half-life of ±Bay K 8644 and the duration of the associated behavioral manifestations [4, 5]. The most notable exception involved the locus coeruleus, suggesting that c-*fos* induction in this region could reflect a combination of both L-type calcium channel activation and a stress response to the behavioral consequences of the drug.

In summary, the regional induction of c-*fos* after the administration of the L-type calcium channel activators, ±Bay K 8644 and FPL 64176, is consistent with the hypothesis that activation of the striatum may be responsible for two main behaviors provoked by these drugs in mice, dystonia and self-injurious biting. Regional microinjections of the drug might be employed to verify this hypothesis. The current results also provide indirect information concerning the anatomical localization of functional L-type calcium channels in the brain.

Acknowledgements

This work was supported by NS01985, NS40470, NS33592, and HD39795.

References

1 Viveros MP, Martin S, Ormazabal MJ, Alfaro MJ, Martin MI: Effects of nimodipine and nifedipine upon behavior and regional brain monoamines in the rat. Psychopharmacology 1996;127:123–132.
2 Cohen C, Perrault G, Sanger DJ: Assessment of the antidepressant-like effects of L-type voltage-dependent channel modulators. Behav Pharmacol 1997;8:629–638.
3 Quartermain D, DeSoria VG, Kwan A: Calcium channel antagonists enhance retention of passive avoidance and maze learning. Neurobiol Learn Mem 2001;75:77–90.
4 Jinnah HA, Sepkuty JP, Ho T, Yitta S, Drew T, Rothstein JD, Hess EJ: Calcium channel agonists and dystonia in the mouse. Mov Disord 2000;15:542–551.
5 Jinnah HA, Yitta S, Drew T, Kim BS, Visser JE, Rothstein JD: Calcium channel activation and self-biting in mice. Proc Natl Acad Sci USA 1999;96:15228–15232.
6 Kasim S, Egami K, Jinnah HA: Self-biting induced by activation of L-type calcium channels in mice: Serotonergic influences. Dev Neurosci 2002;24:322–327.
7 Pothos EN, Davila V, Sulzer D: Presynaptic recording of quanta from midbrain dopamine neurons and modulation of the quantal size. J Neurosci 1998;18:4106–4118.
8 Jankovic J, Fahn S: Dystonic disorders; in Jankovic J, Tolosa E (eds): Parkinson's Disease and Movement Disorders. Baltimore, Williams & Wilkins, 1998, pp 513–551.
9 Visser JE, Baer PR, Jinnah HA: Lesch-Nyhan syndrome and the basal ganglia. Brain Res Rev 2000;32:449–475.
10 Delfs JM, Kelley AE: The role of D_1 and D_2 dopamine receptors in oral stereotypy induced by dopaminergic stimulation of the ventrolateral striatum. Neuroscience 1990;39:59–67.
11 Dickson PR, Lang CG, Hinton SC, Kelley AE: Oral stereotypy induced by amphetamine microinjection into striatum: An anatomical mapping study. Neuroscience 1994;61:81–91.
12 Sharp FR, Sagar SM, Swanson RA: Metabolic mapping with cellular resolution. Crit Rev Neurobiol 1993;7:205–228.
13 Kasim S, Jinnah HA: Self-biting induced by activation of L-type calcium channels in mice: Dopaminergic influences. Dev Neurosci 2003;25:20–25.
14 Campbell DB, Hess EJ: Cerebellar circuitry is activated during convulsive episodes in the tottering *(tg/tg)* mutant mouse. Neuroscience 1998;85:773–783.
15 De Deurwaerdere P, Chesselet MF: Nigrostriatal lesions alter oral dyskinesia and c-*fos* expression induced by the serotonin agonist 1-(*m*-chlorophenyl)piperazine in adult rats. J Neurosci 2000;5170–5178.
16 Litzinger MJ, Grover BB, Saderup S, Abbott JR: Voltage-sensitive calcium channels mark a critical period in mouse neurodevelopment. Int J Dev Neurosci 1993;11:17–24.
17 Tanaka O, Sakagami H, Kondo H: Localization of mRNAs of voltage-dependent Ca^{2+} channels: Four subtypes of α_1- and β-subunits in developing and mature rat brain. Mol Brain Res 1995;30:1–16.
18 Ludwig A, Flockerzi B, Hofmann F: Regional expression and cellular localization of the α_1- and β-subunit of high voltage-activated calcium channels in rat brain. J Neurosci 1997;17:1339–1349.
19 Ahlijanian MK, Westenbroek RE, Catterall WA: Subunit structure and localization of dihydropyridine-sensitive calcium channels in mammalian brain, spinal cord and retina. Neuron 1990;4:819–832.
20 Hell JW, Westenbroek RE, Warner C, Ahlijanian MK, Prystay W, Gilbert MM, Snutch TP, Catterall WA: Identification and differential subcellular localization of the neuronal class C and class D L-type calcium channel α_1-subunits. J Cell Biol 1993;123:949–962.
21 Marangos PJ, Patel J, Miller C, Martino AM: Specific calcium antagonist binding sites in brain. Life Sci 1982;31:1575–1585.
22 Gould RJ, Murphy KMM, Snyder SH: Autoradiographic localization of calcium channel antagonist receptors in rat brain with [^{3}H]nitrendipine. Brain Res 1985;330:217–223.
23 Hirota K, Lambert DG: A comparative study of L-type voltage sensitive Ca^{2+} channels in rat brain regions and cultured neuronal cells. Neurosci Lett 1997;223:169–172.
24 Murphy TH, Worley PF, Baraban JM: L-type voltage-sensitive calcium channels mediate synaptic activation of immediate early genes. Neuron 1991;7:625–635.
25 Westenbroek RE, Sakurai T, Elliott EM, Hell JW, Starr TVB, Snutch TP, Catterall WA: Immunochemical identification and subcellular distribution of the α_{1A}-subunits of brain calcium channels. J Neurosci 1995;15:6403–6418.
26 Nakamura K, Bindokas VP, Kowlessur D, Elas M, Milstien S, Marks JD, Halpern HJ, Kang UJ: Tetrahydrobiopterin scavenges superoxide in dopaminergic neurons. J Biol Chem 2001;276:34402–34407.